Venturi Flow Simulation in ANSYS Fluent

Mechanic of fluids Course project

Sharif University of Technology

Department of Mechanical Engineering

Instructor:

Dr. M. Kamran

Student:

Mohammad Aldaghi

Student Id:

402102827

Contents

1 Introduction

A Venturi tube is a device used to measure the flowrate of a fluid or to modify its pressure characteristics. It operates based on the Venturi effect, which is the reduction in fluid pressure that results when a fluid flows through a constricted section (or choke) of a pipe. According to the continuity equation, as the cross-sectional area of the pipe decreases, the fluid velocity must increase.

Simultaneously, Bernoulli's principle states that this increase in velocity is accompanied by a decrease in static pressure. A standard Venturi tube consists of a converging section, a throat (the narrowest point), and a diverging section where the flow returns to its original diameter.

2 Problem Setup

2.1 Geometry

The geometry of the Venturi tube was created according to the dimensions provided in the project description. The model consists of a converging section, a throat, and a diverging section.

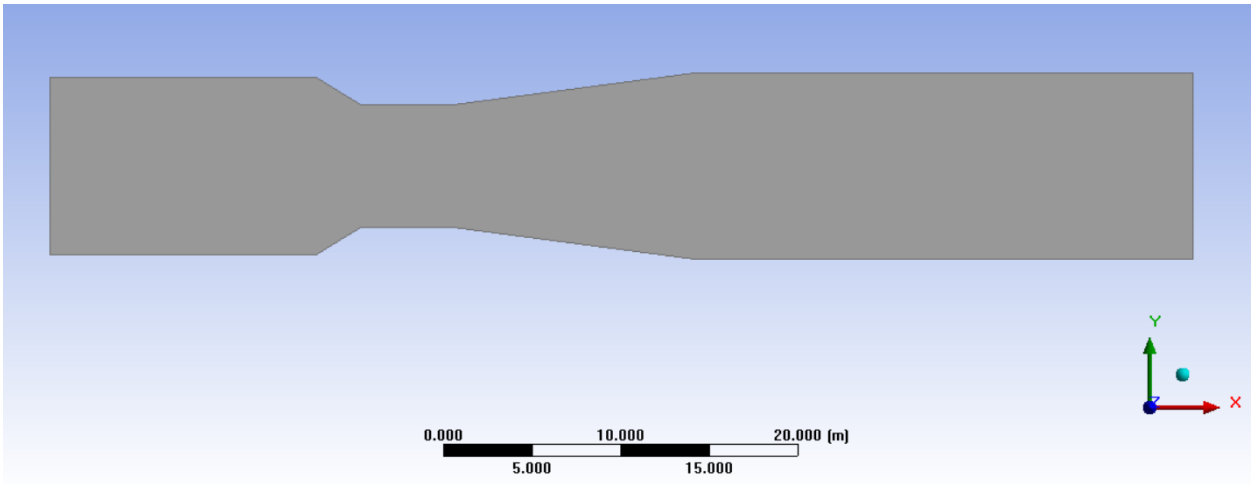

Figure 1. geometry of the venturi tube

2.2 Assumptions

- Steady flow
- Steady state
- Incompressible fluid
- Laminar flow

2.3 Boundary Conditions

A velocity inlet boundary condition was applied at the inlet, while a pressure outlet with zero gauge pressure was specified at the outlet. All walls were modeled as no-slip boundaries.

3 Mesh Generation

The computational domain was discretized using a structured quadrilateral mesh. To accurately capture the flow behavior in the throat region, the mesh density was increased near the converging and diverging sections. Several mesh levels were generated to investigate mesh independence.

3.1 Mesh type

A structured quadrilateral mesh was used for the entire computational domain. The mesh was generated in such a way that a smooth transition of element size is achieved from the inlet toward the throat and the outlet sections.

3.2 Mesh Refinement Strategy

To perform the mesh independence study, four different mesh levels were generated. Starting from a coarse mesh, the number of elements was systematically increased by approximately doubling the number of cells in each refinement step. This approach allows a consistent comparison between different mesh resolutions.

3.3 Mesh Statistics

Mesh Level	Number of Elements
1	2730
2	5580
3	10660
4	20634

Table 1. different number of elements in each Mesh level

These mesh levels were used to evaluate the effect of grid resolution or element size on the predicted pressure of the throat.

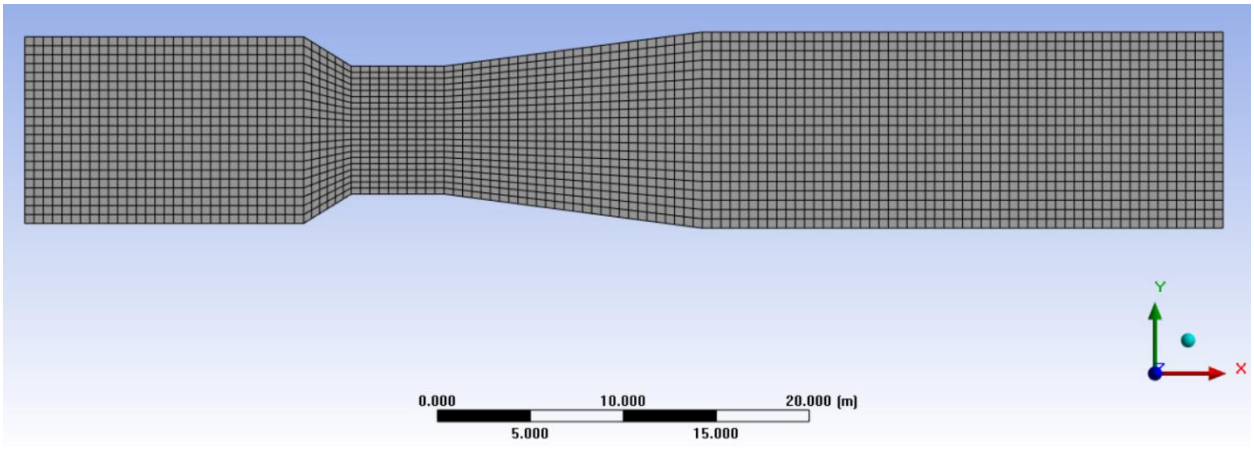

Figure 2. mesh level 1

4 Mesh Independency Studies

A mesh independence study was conducted to ensure that the numerical results are not affected by the grid resolution. The area-weighted average static pressure at the throat was selected as the comparison parameter.

4.1 Comparison Parameter

The area-weighted average static pressure at the throat was used as the main parameter for evaluating mesh independence. This quantity was extracted for all mesh levels and compared as the mesh was refined.

4.2 Mesh Independency Results

Mesh Level	Number of Elements	Pressure [Pa]
1	2730	-0.019339232
2	5580	-0.020423914
3	10660	-0.020997888
4	20634	-0.021359325

Table 2. Pressure for each Mesh level

As the mesh is refined, the throat static pressure converges. The variation between Mesh 3 and Mesh 4 is less than 2%, indicating mesh independence. Therefore, Mesh 4 was selected for all subsequent simulations.

4.3 Mesh Independence Plot

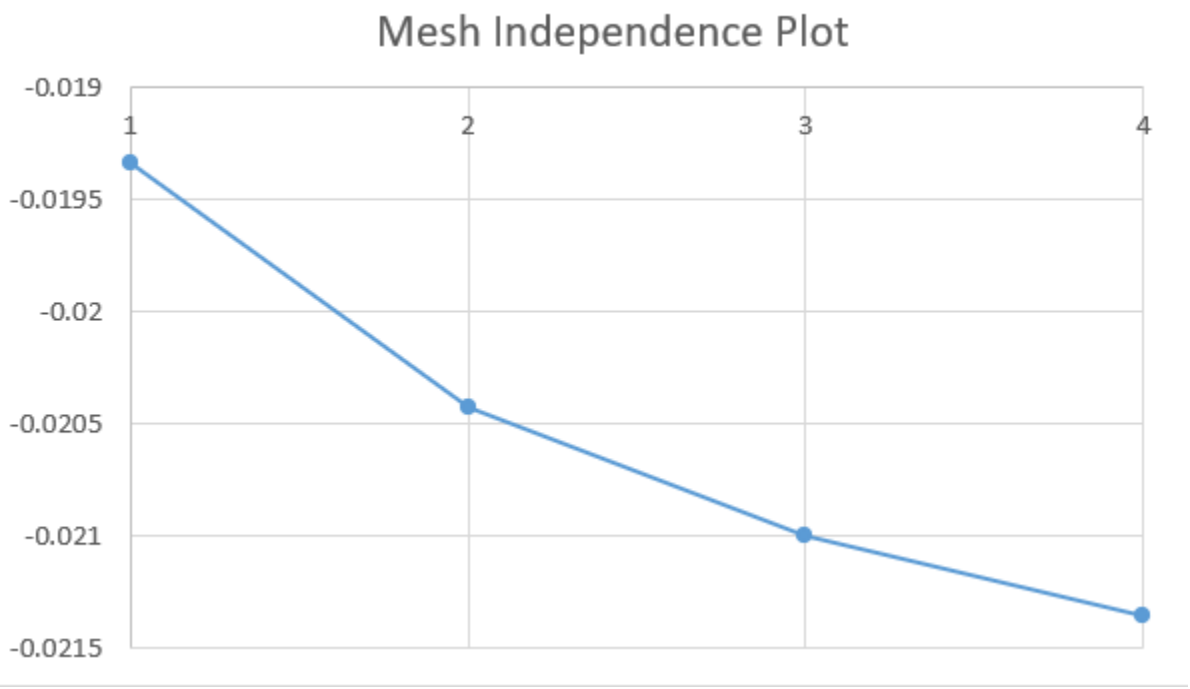

Plot 1. Mesh Independence on Mesh level 4

5 CFD Results

In this section, the numerical results obtained from the CFD simulations using the selected mesh are presented and the contours of various parameters.

5.1 Pressure Contour

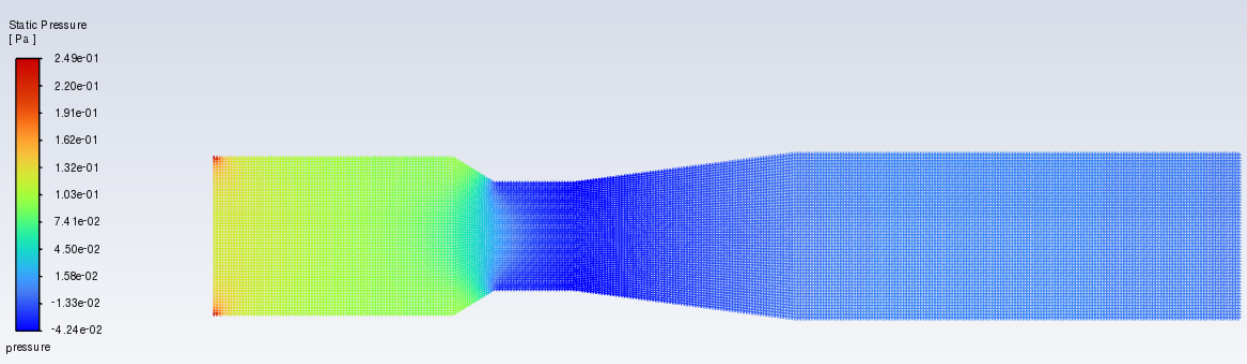

Figure 3. Static pressure contour

Figure 3 shows the static pressure contour for the selected mesh. A significant pressure drop is observed at the throat, while pressure recovery occurs in the diverging section.

5.2 Velocity Contour

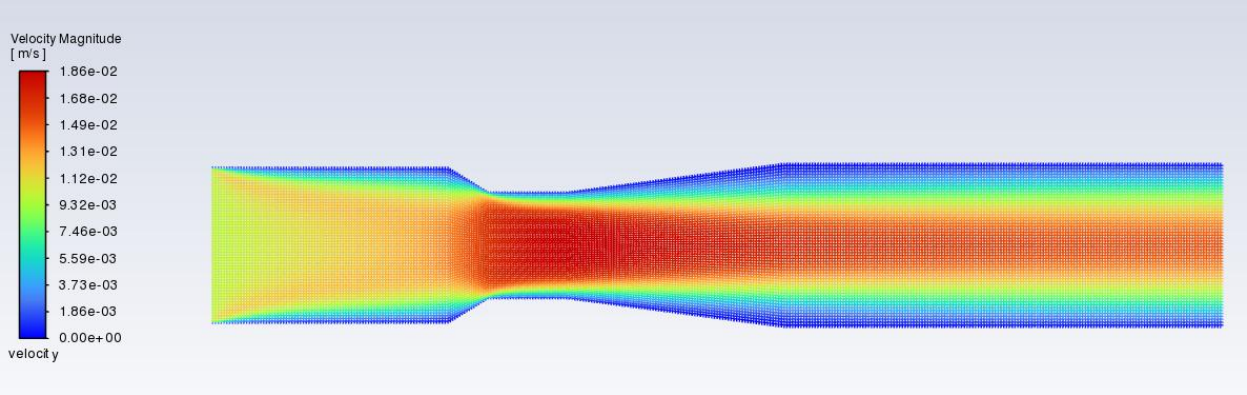

Figure 4. Velocity contour

The velocity contour shows zero velocity at the walls due to the no-slip boundary condition. The velocity increases toward the centerline and reaches a maximum value at the throat, which is consistent with viscous internal flow behavior and the continuity equation.

5.3 Pathline

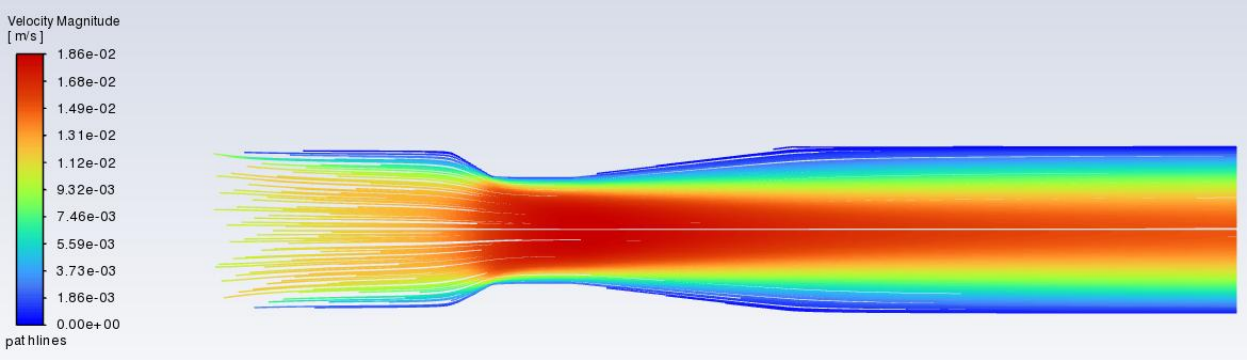

Figure 5. Pathline colored by velocity magnitudes

5.4 Reynolds number contour

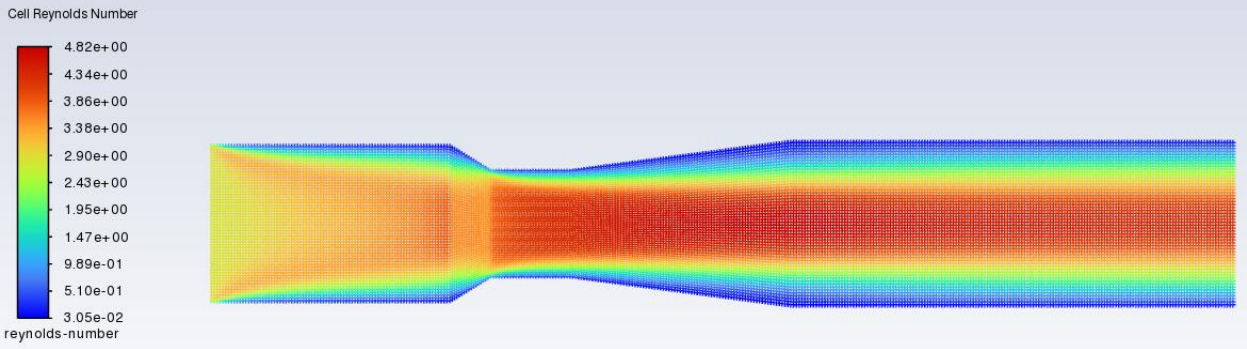

Figure 6. Reynolds number contour

Figure 6 shows the contour of the Reynolds number for the selected mesh. The maximum Reynolds number in the computational domain is approximately **Re ≈ 4.82**, which occurs at the throat region where the fluid velocity reaches its highest value.

6 Analysis and Discussions

In this section, the numerical results obtained from the CFD simulations are analyzed and compared with theoretical predictions from fluid mechanics. The effects of continuity, viscous losses, and modeling assumptions are discussed to evaluate the physical consistency and accuracy of the simulation results.

6.1 Velocity Verification (Continuity Equation)

For continuity equation we have:

$$A_1 V_1 = A_2 V_2$$

And for diameter of the outlet, we have:

$$d = 2 \times (5 - 3\sin(31.6) + 14\sin(7.5)) = 10.51$$

So for out let velocity we have:

$$V_2 = (\frac{10}{10.51})^2 \times 0.01 = 0.0091$$

The CFD results show that the area-weighted average outlet velocity is approximately **0.00951 m/s**, which is in good agreement with the analytically calculated value. This confirms that mass conservation is satisfied in the numerical simulation.

6.2 Pressure Recovery and Viscous Losses

The pressure contour in the diverging section of the Venturi tube shows partial pressure recovery downstream of the throat. However, the outlet pressure does not fully return to the inlet pressure level.

This incomplete pressure recovery is caused by viscous losses and energy dissipation within the flow. Unlike the ideal flow assumption, real viscous flows experience frictional losses, which reduce the mechanical energy of the fluid and prevent full pressure recovery.

6.3 Bernoulli vs. CFD

For analytical section and Bernoulli equation we have:

$$\frac{1}{2}\rho V_1^2 + P_1 = \frac{1}{2}\rho V_2^2 + P_2$$

For velocity of throat, we have:

$$A_1 V_1 = A_2 V_2$$

And for diameter of the throat:

$$d = 2 \times (5 - 3\sin(31.6)) = 6.856$$

So:

$$V_2 = (\frac{10}{6.856})^2 \times 0.01 = 0.0213$$

And if we consider the difference or pressures between inlet and throat we have:

$$\Delta P = \frac{1}{2} \times 1260 \times (0.01^2 - 0.0213^2) = 0.222 \text{ [Pa]}$$

The analytical Bernoulli prediction results in a pressure drop of approximately **0.222 Pa**, whereas the CFD simulation yields a smaller pressure drop of approximately **0.156 Pa**. Therefore, the pressure drop predicted by the CFD simulation is **smaller** than the theoretical value obtained from Bernoulli's equation.

This discrepancy arises from the assumptions inherent in Bernoulli's equation. The analytical model assumes inviscid flow and a uniform velocity profile at the throat, which leads to a higher estimated throat velocity and consequently a larger pressure drop. In contrast, the CFD result is based on an area-weighted average velocity and accounts for viscous effects and non-uniform velocity distribution across the throat cross-section.

As a result, the CFD simulation provides a more realistic representation of the actual flow behavior, while Bernoulli's equation serves as an idealized upper-bound estimate of the pressure drop.

6.4 Validity of Laminar Assumption

The Reynolds number contour obtained from the CFD simulation was examined to assess the validity of the laminar flow assumption. The maximum Reynolds number in the computational domain occurs at the throat region, where the fluid velocity reaches its highest value. The maximum Reynolds number was found to be approximately **Re ≈ 4.82**.

This value is significantly lower than the critical Reynolds number for transition to turbulence in internal pipe flow. Therefore, the flow remains entirely within the laminar regime throughout the domain, and the assumption of laminar flow in this simulation is fully justified.

If the Reynolds number were to exceed the critical value, the laminar flow model would no longer be appropriate, and neglecting turbulence effects could lead to inaccurate predictions of velocity and pressure distributions. In such a case, a suitable turbulence model would be required to correctly capture the flow behavior.

7 Conclusion

In this project, the flow through a Venturi tube was simulated using ANSYS Fluent. A mesh independence study was conducted to ensure the reliability of the numerical results, and an appropriate mesh was selected for the final simulations.

The CFD results demonstrated physically consistent behavior, including pressure drop at the throat, velocity increase due to area reduction, and partial pressure recovery in the diverging section. Comparison with analytical predictions based on Bernoulli's equation showed reasonable agreement, while highlighting the effects of viscous losses and non-uniform velocity distribution.

The Reynolds number analysis confirmed that the flow remained within the laminar regime, validating the laminar flow assumption used in this study. Overall, the numerical results were found to be consistent with fundamental fluid mechanics principles.